

**Constraints on the Horizontal-Branch Morphology
of the Globular Cluster M79 (NGC 1904)
from Optical and Far-UV Observations**

W. Van Dyke Dixon and Arthur F. Davidsen
Department of Physics and Astronomy, The Johns Hopkins University
3400 N. Charles Street, Baltimore, Maryland 21218
wvd@pha.jhu.edu, afd@pha.jhu.edu

Ben Dorman
Laboratory for Astronomy and Solar Physics, Code 681
NASA Goddard Space Flight Center, Greenbelt, MD 20771
dorman@shemesh.gsfc.nasa.gov

and

Henry C. Ferguson
Space Telescope Science Institute, Baltimore, MD 21218
ferguson@stsci.edu

Version of December 29, 2017

ABSTRACT

The globular cluster M79 was observed with the Hopkins Ultraviolet Telescope (HUT) during the Astro-1 space shuttle mission in 1990 December. The cluster's far-UV integrated spectrum shows strong absorption in the Lyman lines of atomic hydrogen. We seek to use this spectrum, together with optical photometry, to constrain the stellar mass distribution along its zero-age horizontal branch (ZAHB). We find that a Gaussian distribution of ZAHB masses, with a mean of $0.59M_{\odot}$ and standard deviation $0.05M_{\odot}$, is able to reproduce the cluster's (B, V) color-magnitude diagram when subsequent stellar evolution is taken into account, but cannot reproduce the cluster's far-UV spectrum. Model stellar spectra fit directly to the HUT data indicate a surprising distribution of atmospheric parameters, with surface gravities (and thus implied masses) significantly lower than are predicted by canonical HB evolutionary models. This result is consistent with the findings of Moehler et al. [A&A, 294, 65 (1995)] for individual HB stars in M15. Further progress in understanding the mass distribution of the HB must await resolution of the inconsistencies between the derived stellar atmospheric parameters and the predictions of HB evolutionary models. Improved stellar spectral models, with higher spectral resolution and non-solar abundance ratios, may prove useful in this endeavor.

Subject headings: globular clusters: general — globular clusters: individual (M79) — stars: horizontal-branch — ultraviolet: stars

1. Introduction

M79 (NGC 1904) is a centrally condensed, intermediate-metallicity ($[\text{Fe}/\text{H}] = -1.69$) globular cluster (Djorgovski & King 1986; Djorgovski 1993) with an extremely blue horizontal branch (Stetson & Harris 1977), extending at its high-temperature end as faint as the main-sequence turnoff (Ferraro et al. 1992). The cluster’s integrated UV spectrum is nearly flat from 1500 to 3300 Å (van Albada et al. 1981), and observations with the Ultraviolet Imaging Telescope (UIT; Hill et al. 1992) indicate that most of the far-UV flux emanates from individual blue HB (BHB) and post-HB stars.

In our current understanding (Renzini 1981), stars with zero-age-main-sequence mass $M_{ZAMS} \sim M_{\odot}$ lose about $0.2M_{\odot}$ while ascending the red-giant branch (RGB) and eventually produce zero-age horizontal branch (ZAHB) stars with core masses $M_C \sim 0.5M_{\odot}$ and envelope masses $M_{env} \sim 0.1M_{\odot}$. A star’s location on the ZAHB is determined by the mass of the hydrogen-rich envelope remaining above the helium-rich core, which for typical globular cluster ages is a function only of the abundances of helium and heavier elements (Y, Z). Stellar evolutionary models imply a spread in M_{env} , with the bluest HB stars having the lowest masses (Dorman et al. 1993).

The mass distributions used to derive gross cluster properties from the HB population are most often based on the function introduced by Rood (1973). This function consists of a Gaussian multiplied by polynomial truncation terms designed to ensure that the simulation contains physically possible objects, i.e., stars with $M_C \leq M \leq M_{RG}$. Otherwise, the assumption is not based on any physical understanding of the cause of the HB mass spread (Rood 1990). Monte-Carlo simulations based on such syntheses have been quite successful in reproducing observed HB morphologies (Rood 1973; Lee et al. 1990, 1994; Catelan 1989); however, the polynomial truncation terms give distributions that are skewed away from the theoretical limits of the mass range, a situation that may not be desirable for the extremely blue HB of M79.

In this paper we analyze the far-UV spectrum of M79 obtained with the Hopkins Ultraviolet Telescope (HUT). Our object is to derive constraints on the ZAHB mass distribution from our far-UV spectrum and from optical photometry. Ferraro et al. (1992) note that the distribution of stars in the color-magnitude diagram (CMD) of M79 seems quite different from a Gaussian. We investigate whether a Gaussian distribution of masses along the ZAHB can reproduce this asymmetry by combining the HB evolutionary models of Dorman et al. (1993) with the synthetic stellar flux distributions of Kurucz (1992) to fit the cluster’s optical CMD (Ferraro et al. 1992). We find that a Gaussian distribution of ZAHB masses with a mean of $0.59M_{\odot}$ and standard deviation $0.05M_{\odot}$ can indeed reproduce the cluster’s CMD. We use this model to compute synthetic far-UV spectra using a Monte Carlo algorithm, compare them with the HUT spectrum, and find that it cannot reproduce the observed far-UV flux distribution. Using individual Kurucz model flux distributions, we derive surface gravities for BHB stars that are significantly lower than theoretical predictions. This result is consistent with that of Moehler et al. (1995) for individual HB stars in M15. We conclude that more precise constraints on the HB mass distribution must await a resolution of this discrepancy.

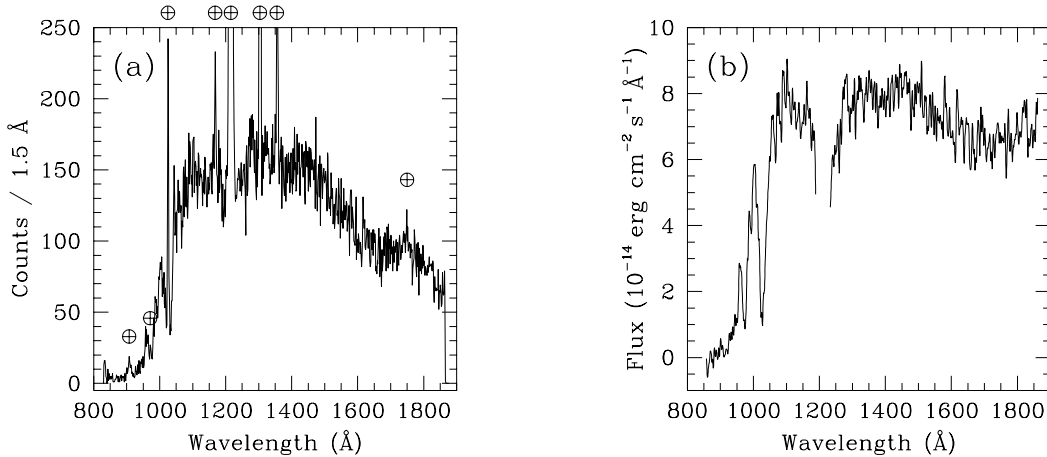


Fig. 1.— (a) HUT spectrum of M79 in raw counts, binned by three pixels (about 1.5 Å) and uncorrected for airglow or extinction. Airglow features are marked with ⊕. (b) Flux-calibrated, airglow-subtracted spectrum of M79. The spectrum has been dereddened with a Cardelli et al. (1989) extinction curve, assuming $E(B - V) = 0.01$ and $R_V = 3.1$, and smoothed with a Gaussian to 3.0 Å resolution.

2. Observations and Data Reduction

The spectrum of M79 was obtained with HUT on the Astro-1 mission of the space shuttle *Columbia* in 1990 December. HUT consists of a 0.9-m mirror that feeds a prime-focus spectrograph with a microchannel-plate intensifier and photo-diode array detector. First-order sensitivity covers the region from 830 to 1850 Å at 0.51 Å pixel⁻¹ with about 3 Å resolution. The spectrograph and telescope are described in detail by Davidsen et al. (1992). Two observations of M79 were obtained during orbital night through a 9'' × 116'' aperture, with a total integration time of 2366 s. The first observation, of 764 s duration, was begun on 1990 December 5 at UT 15:33:47; the second, for 1602 s, was obtained two orbits later, beginning at UT 18:33:45. During both observations, the aperture was centered on the cluster center of light. The pointing stability was quite good: 1.0'' rms in both pitch and yaw for the 1602 s observation and 1.4'' and 1.8'' rms, respectively, in pitch and yaw for the 764 s pointing. (Pitch corresponds to the short dimension of the HUT aperture, yaw to the long dimension.) The combined spectrum, presented in Fig. 1a, shows strong absorption by atomic hydrogen, but no emission features other than well-known geocoronal lines.

In order to estimate the contribution of the earth’s residual atmosphere to the observed spectrum, emission-line profiles were fit to an airglow spectrum taken during orbital night through the same aperture as the M79 observations. These airglow line profiles were combined with a linear continuum and fit to the region around each airglow line in the cluster spectrum. The line profiles were held fixed while their fluxes were allowed to vary. Exception was made for the $\text{Ly}\beta$ and γ airglow lines, for which a Gaussian absorption feature was included in the continuum-plus-airglow model that was fit to the data, and the complex of N I and N II airglow features between 903 and 916 Å, for which the model line shapes, as well as the fluxes, were allowed to vary in fitting the cluster spectrum. The resulting synthetic airglow spectrum was subtracted from the cluster spectrum. This procedure led to an oversubtraction of the core of $\text{Ly}\alpha$; regions around this line were omitted from subsequent model fits to the spectra. The airglow lines subtracted are marked in Fig. 1a.

Once airglow-subtracted, the spectrum was scaled to correct for pulse-persistence effects. A constant dark-current contribution was subtracted, as was scattered light from the grating, determined from the count rate between 850 and 895 Å, a region free from airglow and stellar emission. The second-order contribution from wavelengths longward of 912 Å, which affects fluxes longward of 1824 Å, was also scaled and subtracted. The raw-counts spectrum was converted to physical units using the HUT absolute calibration, based on a model atmosphere of the white dwarf G191-B2B. Comparison with pre-flight and post-flight laboratory measurements indicates that the calibration is accurate to approximately 5% over all wavelengths (Davidsen et al. 1992; Kimble et al. 1993; Kruk et al. 1996). Errors for each channel were estimated assuming Gaussian statistics and were propagated through the data-reduction process. The flux-calibrated, airglow-subtracted HUT spectrum of M79 is presented in Fig. 1b. For this figure (only), the spectrum has been dereddened with a Cardelli et al. (1989) curve, assuming $E(B-V) = 0.01$ and $R_V = 3.1$, and smoothed with a Gaussian to 3.0 Å resolution.

The exact position of the HUT aperture is shown in Fig. 2a, a far-UV image of the cluster obtained by UIT (Hill et al. 1992). Two UV-bright stars discovered by UIT are circled. Hill et al. estimate that M79 contains a total of 220 ± 10 HB stars. From Fig. 2a, we estimate that 20 to 40 of these stars fall within the HUT aperture. Also shown is the location of the *International Ultraviolet Explorer’s* (IUE) large aperture during an observation made by Altner & Matilsky (1993). Their analysis indicates the presence of a UV-bright star at the edge of the HUT aperture, near the southeastern intersection of the HUT and IUE apertures. A second UV-bright star found by Altner & Matilsky is much fainter and lies outside the HUT aperture. These objects were not known at the time of the Astro-1 flight.

Ferraro et al. (1992) provide positional information, colors, and magnitudes for stars farther than 15'' from the center of M79. A map based on their positions of the cluster’s HB stars is presented in Fig. 2b. Note the correspondence between this map and the UIT image; most of the stars resolved with UIT were observed by Ferraro et al. A CMD for the complete sample of approximately 200 HB stars in M79, statistically corrected for contamination by field stars, is presented in Fig. 3a.

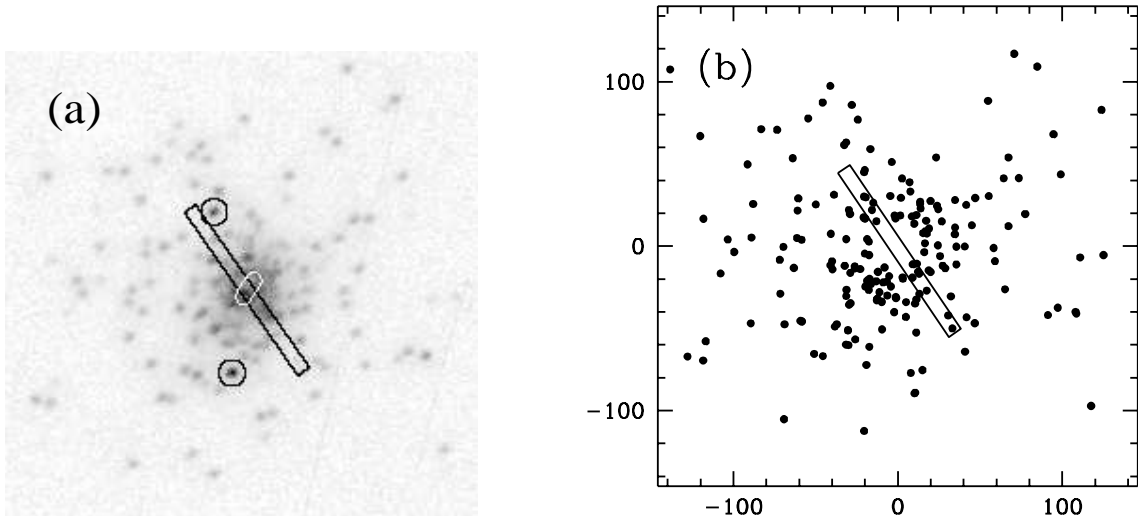


Fig. 2.— (a) Far-UV image of M79 obtained with the Ultraviolet Imaging Telescope (UIT; Hill et al. 1992). North is up and east is to the left. The position of the HUT aperture is marked in black, and that of the *IUE* aperture (Altner & Matilsky 1993) in white. For scale, the length of the HUT aperture is $116''$. Two UV-bright stars discovered by Hill et al. are circled. The UV-bright star discovered by Altner & Matilsky lies near the southeastern intersection of the HUT and *IUE* apertures. (b) Map showing the positions of HB branch stars of M79 drawn from the data of Ferraro et al. (1992). Units are arc seconds from the cluster center.

3. Fitting the Optical CMD

We have used the formulation of Lee et al. (1990) in fitting a Gaussian HB mass-distribution model to the optical CMD of M79 (Ferraro et al. 1992). This model assumes that stars on the ZAHB have a Gaussian distribution in mass $P(M)$ resulting from variable amounts of mass loss on the RGB:

$$P(M) \propto [M - (\langle M_{HB} \rangle - \Delta M)] (M_{RG} - M) \exp \left\{ - \left(\frac{\langle M_{HB} \rangle - M}{\sigma} \right)^2 \right\}, \quad (1)$$

where $M_{RG} = 0.80M_{\odot}$ is the mass a star would have at the tip of the RGB if it did not lose mass (assuming a cluster age of about 15 Gyr), $\Delta M = M_{RG} - \langle M_{HB} \rangle$ is the mean amount of mass loss, and σ is the mass dispersion. The mass distribution is truncated at M_{RG} at the high-mass end and at $\langle M_{HB} \rangle - \Delta M$ at the low-mass end (see inset of Fig. 4a). For most clusters, $\langle M_{HB} \rangle - \Delta M$ is greater than M_C , but the

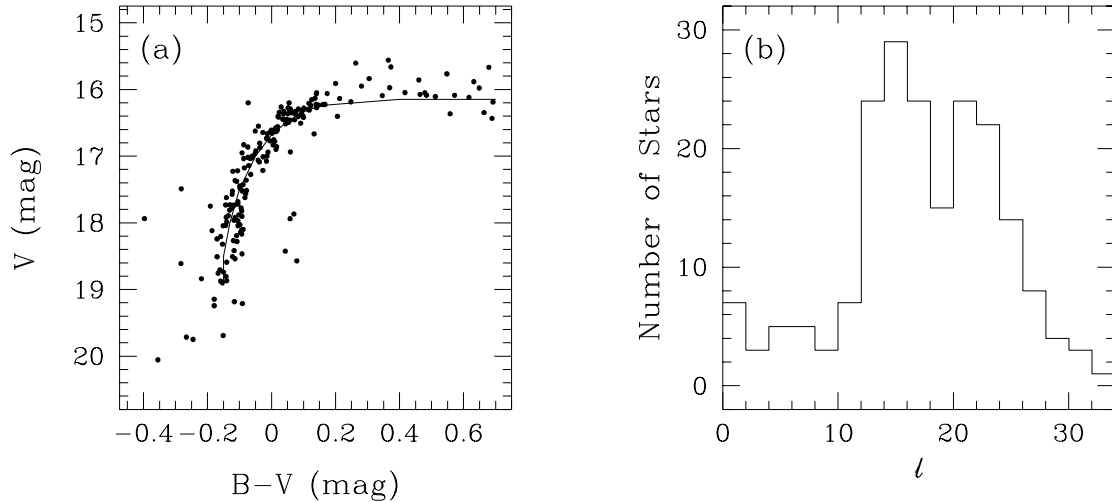


Fig. 3.— (a) Color-magnitude diagram (CMD) of the approximately 200 HB stars observed by Ferraro et al. (1992). The ridge line for the cluster is also shown. (b) The observed distribution of stars along the HB in M79. $l \equiv 0$ at $V = 16.15$ and $B - V = 0.70$ and increases to the blue along the ridge line.

HB of M79 is so blue that $P(M)$ predicts a finite number of stars with mass less than M_C . These stars, representing only one or two percent of the total population, are simply ignored in our analysis.

To produce a model HB, 10 000 stars are selected with masses distributed according to the probability distribution $P(M)$ and ages chosen from a set of uniform random deviates between 0 and 1.4×10^8 years. We ignore variations in the main-sequence turn-off mass ($< 0.002M_\odot$; Castellani 1980) over this time scale. Given the stellar mass and age, we use the HB evolutionary models of Dorman et al. (1993) to determine the temperatures and surface gravities of the evolving HB and post-HB stars. These models assume $[\text{Fe}/\text{H}] = -1.48$, $[\text{O}/\text{Fe}] = 0.60$, and a core mass of $0.485 M_\odot$. Stellar magnitudes and colors are then interpolated from the grid of synthetic stellar flux distributions computed by Kurucz (1992) for stars with an abundance $[\text{M}/\text{H}] = -1.5$, assuming a distance modulus of $(m - M)_0 = 15.65$ (Harris & Racine 1979).

In order to provide a purely empirical measure of the stellar distribution along the HB, Ferraro et al. (1992) define a coordinate “ l ” (similar to X_{HB} in the coordinate system of Rood & Crocker 1989) that is linear along the ridge line of the HB, divide the whole length into equal bins, and count the stars populating each bin, perpendicular to the ridge line (see their Figs. 12 and 13; the technique is described fully by

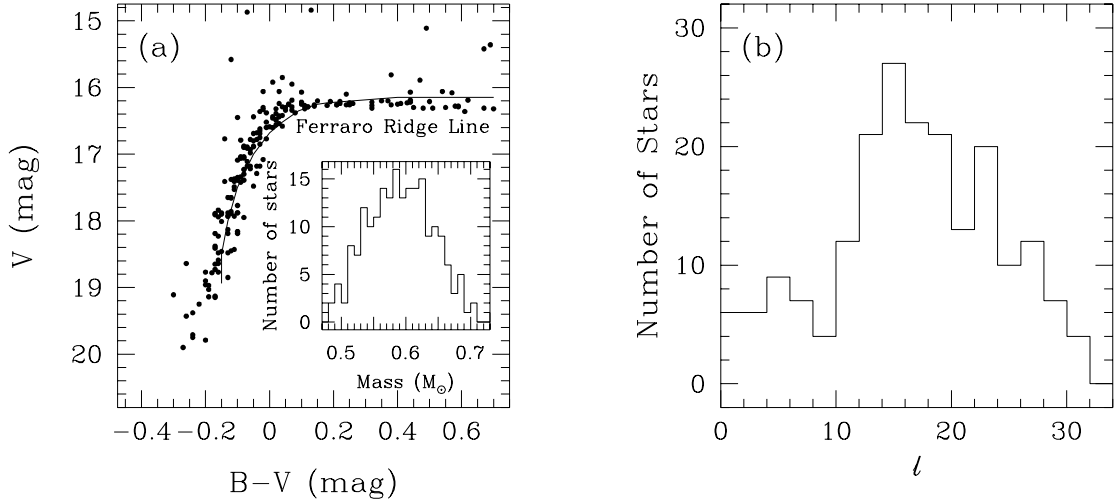


Fig. 4.— (a) A synthetic color-magnitude diagram (CMD) showing 200 model stars drawn from the best-fitting Gaussian HB mass distribution. (Stars that have evolved redward of $B-V = 0.7$ are not shown.) The observed HB ridge line is plotted for comparison. *Inset*: The distribution of mass among the HB stars in this model. (b) The HB distribution of the best-fitting Gaussian model.

Fusi Pecci et al. 1993). We have attempted to implement this process in software; the resulting distribution is presented in Fig. 3b. Note the asymmetric shape: the l distribution is skewed toward the blue. While noting that each bin in l space may not correspond to an equal interval in effective temperature, Ferraro et al. argue that the stellar distribution along the HB is not Gaussian.

To determine the values of $\langle M_{HB} \rangle$ and σ that best reproduce the HB of M79, we compute a grid of HB models, incrementing $\langle M_{HB} \rangle$ and σ in steps of $0.01 M_{\odot}$. Colors and magnitudes of the resulting model HB stars are scattered according to the observational errors estimated by Ferraro et al. (1992). For each mass-distribution model, we compute 10 000 model stars, divide them into samples of 200 each, and determine the l distribution for each sample, ignoring models that have evolved redward of $B-V = 0.70$. We compare the l distribution of each sample with that of the Ferraro et al. data, using the Kolmogorov-Smirnov (KS) test (Press et al. 1988) to determine the probability Q_{KS} that the model and data are drawn from the same parent population. By rejecting HB models with $\langle Q_{KS} \rangle < 0.01$, we can exclude models with $\langle M_{HB} \rangle < 0.56$ and $\langle M_{HB} \rangle > 0.61$ at the 99% confidence level. With $\langle Q_{KS} \rangle = 0.37$, the best-fitting model has $\langle M_{HB} \rangle = 0.59 M_{\odot}$ and $\sigma = 0.08 M_{\odot}$. Because the Gaussian distribution is

truncated at both ends, the mass dispersion parameter in Equation (1) is approximately a factor of two larger than the actual standard deviation of the mass dispersion, which Lee et al. (1990) call σ_{SD} . For our model, $\sigma_{SD} = 0.05M_{\odot}$.

A synthetic CMD and a plot of the l distribution for 200 HB stars selected from the best-fitting model are presented in Fig. 4. The mass distribution of the HB stars in this model is also shown. This (nearly) Gaussian mass distribution is remarkably successful at reproducing the non-Gaussian distribution in the parameter l observed by Ferraro et al. (1992). The transformation from a Gaussian distribution of initial masses to a skewed distribution of stars along the HB reflects an evolutionary effect of the Dorman et al. (1993) tracks: stars with $M \lesssim 0.50M_{\odot}$ evolve to higher luminosities at nearly constant temperature, while those with higher masses cool rapidly, driving the l distribution sharply toward the red.

The model HB seems to be about 0.2 magnitudes brighter than the cluster ridge line at $B-V = 0$ and about 0.2 magnitudes fainter at $B-V = 0.4$. These discrepancies may reflect small errors in the evolutionary or stellar atmosphere models combined with uncertainties in the cluster’s distance modulus. We have repeated the optical CMD fit assuming a variety of cluster distances and find that the parameters of the best-fitting model do not change over the range $15.60 \leq (m - M)_0 \leq 15.70$.

4. Fitting the Far-UV Spectrum

4.1. The Gaussian Model

To determine whether the Gaussian mass-distribution model that best fits the optical CMD of M79 is able to reproduce its far-UV spectrum, we use a Monte Carlo procedure to construct synthetic cluster spectra. We select stars at random from our best-fitting model HB, compute their far-UV spectra from the nearest Kurucz (1992) model in $\log g - T_{eff}$ space, and sum them until the model flux between 900 and 1768 Å equals the HUT flux in this range. By computing the far-UV spectra for 1000 realizations of this random sampling of the HB mass distribution, we can accurately assess the probability that the observed spectrum could have been obtained from the model HB distribution.

The Kurucz (1992) models have a resolution of about 10 Å, incorporate statistically correct line strengths for 58 million atomic and molecular transitions, and are available for scaled solar abundances $1.0 \gtrsim [M/H] \gtrsim -5.0$. The models provide a thorough treatment of line blanketing by metals, though Kurucz’s assumption of local thermodynamic equilibrium (LTE) is inappropriate for stars with high effective temperatures or low surface gravities. Fortunately, non-LTE effects are small for stars on the HB (Kudritzki 1979, 1990).

Our observed spectrum is binned by 20 pixels to bring it to the 10 Å resolution of the Kurucz models. Model spectra are fit to the data using the non-linear curve-fitting program “specfit” (Kriss 1994), a χ^2 minimization routine running in the IRAF¹ environment. The only free parameter in the fit is the

¹The Image Reduction and Analysis Facility (IRAF) is distributed by the National Optical Astronomy Observatories, which

normalization of the model. To model the effects of interstellar reddening, the program uses a Cardelli et al. (1989) extinction curve, assuming $E(B-V) = 0.01$ (Peterson 1993) and $R_V = 3.1$. A neutral-hydrogen absorption model assuming a Doppler velocity parameter of 10 km s^{-1} is included in the fit, for which the column density toward M79 is determined by integrating a 21-cm spectrum from the survey of Stark et al. (1992) through the velocity range -100 km s^{-1} to $+100 \text{ km s}^{-1}$, with a result of $N_H = 5.307 \times 10^{19} \text{ cm}^{-2}$. Within specfit, the models are interpolated to the exact wavelengths of the data points; this resampling may introduce small errors in the model flux.

In the rebinned spectrum of M79, the signal-to-noise ratio ranges between 20:1 and 30:1 at wavelengths longer than about 1000 \AA . The uncertainty in the HUT absolute calibration is estimated to be about 5% on scales of roughly 50 \AA . Because the systematic errors are comparable to the random statistical errors, it is necessary to relax the standard χ^2 criterion for goodness of fit. As a guide to how well Kurucz (1992) models can fit HUT spectra, we consider the individual globular-cluster UV-bright stars studied by Dixon et al. (1994). For those stars, the best-fitting models yield $\chi^2 = 195.0$ for $\nu = 88$ and $\chi^2 = 219.5$ for $\nu = 87$, respectively. We will thus consider an acceptable spectrum to be one with $\chi^2 < 200$ and exclude as unacceptable any ensemble of stars that does not yield $\chi^2 < 200$ in at least 5% (50 of 1000) of its spectra. There are 83 data points in the rebinned M79 spectrum.

A UV-bright star discovered with *IUE* by Altner & Matilsky (1993) lies at the edge of the HUT aperture (Fig. 2a). The authors estimate the star to have $T_{eff} = 13\,000 \text{ K}$, $\log g = 3.3$, and solar abundance. Its abundance is important, for though changes in metallicity have only a minor effect on the flux of Kurucz (1992) models longward of 1200 \AA , line blanketing by metals can vastly alter the apparent continuum level at shorter wavelengths. *IUE* spectra have a short-wavelength cutoff of about 1200 \AA , while HUT spectra continue to the Lyman limit, revealing the extreme sensitivity of the sub- $\text{Ly}\alpha$ continuum to metal-line opacity in stellar atmospheres. Dixon et al. (1994, 1995) fit Kurucz (1992) models to HUT spectra of three UV-bright stars in globular clusters. In each case, a Kurucz model with the cluster metallicity provides a significantly better fit to the data than the best fitting solar-metallicity model. We thus include a model spectrum of a star with $T_{eff} = 13\,000 \text{ K}$, $\log g = 3.3$ (interpolated from $\log g = 3.0$ and 3.5 models), and $[M/H] = -1.5$ in each of our synthetic spectra.

We seek to model only the BHB of M79. From its CMD (Fig. 3a), we see that the red end of the cluster’s BHB lies at $B-V \sim 0.15$, corresponding to stellar temperatures of about 7500 K . Because Kurucz (1992) models with $T_{eff} \lesssim 7500 \text{ K}$ do not emit significant flux at wavelengths shortward of 1770 \AA , and because the HUT spectrum of M79 rises at longer wavelengths, reflecting the contribution of stars at the main-sequence turn-off to the integrated cluster flux, we exclude this region ($\lambda > 1770 \text{ \AA}$) from our analysis.

We construct 1000 synthetic spectra from the 10 000 stars in our model HB population using the above algorithm and compute χ^2 for each spectrum. We find that the best-fitting 5% of the models have

values of $\chi^2 < 426$ ($\nu = 81$) and the best-fitting model has $\chi^2 = 307$. Its spectrum is presented in Fig. 5. We see that the model predicts a Ly α absorption feature considerably broader than is shown by the data. Indeed, most of the contribution to χ^2 comes from the regions around the Ly α and β absorption lines. To verify that this discrepancy does not reflect uncertainties in the Ly α airglow subtraction, we extract about 1300 s of data from the darkest part of orbital night, when the Ly α airglow emission is lowest and the Ly α absorption feature least obscured. To these data, we fit a three-component model, with a linear continuum, a Gaussian absorption feature, and a model Ly α airglow profile. The idea is less to constrain uniquely the relative strengths of the Ly α absorption and emission features than to maximize the contribution of the model Ly α airglow line. When this model airglow feature is subtracted from the data, we find no significant change in the resulting absorption line profile, indicating that the discrepancy between the model and the data is not due to errors in our airglow subtraction. We conclude that the Gaussian mass distribution that best fits the optical CMD of M79 is unable to reproduce its far-UV spectrum. Hereafter, we shall refer to this distribution of stars as the Gaussian model.

4.2. The Empirical Model

We have found that a Gaussian distribution of ZAHB masses is able to reproduce the CMD of M79, but not its far-UV spectrum. Is this failure a reflection of errors in our ZAHB mass distribution, or does it point to more subtle problems in our model? To address this question, we first attempt to reproduce the cluster’s far-UV flux distribution using a simple collection of Kurucz (1992) stellar atmosphere models. We find that the HUT spectrum of M79 can be reproduced using only four Kurucz model spectra, all with $[M/H] = -1.0$. The models have $T_{eff} = 8500, 11\ 000, 15\ 000,$ and $27\ 000$ K, and $\log g = 3.0, 3.5, 4.0,$ and 3.5 , respectively. Generally speaking, these four spectra provide flux in the regions (1) longward of about $1500\ \text{\AA}$, (2) between $1500\ \text{\AA}$ and Ly α , (3) between Ly α and Ly γ , and (4) shortward of Ly γ , respectively. We find that $\chi^2 = 148$ ($\nu = 73$) for this model, making $\chi^2_\nu = 2.0$. The resulting synthetic spectrum is plotted in Fig. 6 (dashed line).

We next construct a model stellar population based on this distribution of stellar parameters and compare it with the data. For each HB star observed by Ferraro et al. (1992), we select a Kurucz (1992) model spectrum with $[M/H] = -1.0$. We choose T_{eff} to match the observed $B - V$, then select $\log g$ according to the following scheme: for stars with $T_{eff} < 9750$ K, models with $\log g = 3.0$ are selected; for those with $9750 < T_{eff} < 13\ 000$ K, $\log g = 3.5$; for stars with $13\ 000 < T_{eff} < 20\ 000$ K, $\log g = 4.0$; and for $T_{eff} > 20\ 000$ K, $\log g = 3.5$. The flux is scaled to match the observed V magnitude. Four stars with measured $B - V < -0.3$ are excluded from our sample, as their colors are probably erroneous. Such hot stars would be prominent in the UIT image, yet only one of them was seen, and its UV color indicates a much lower temperature.

From this ensemble of approximately 200 model stellar spectra, we generate 1000 synthetic cluster spectra, each including the Altner & Matilsky (1993) UV-bright star (though now with an assumed metallicity of $[M/H] = -1.0$), and compare them with our data. The minimum value of χ^2 that we achieve

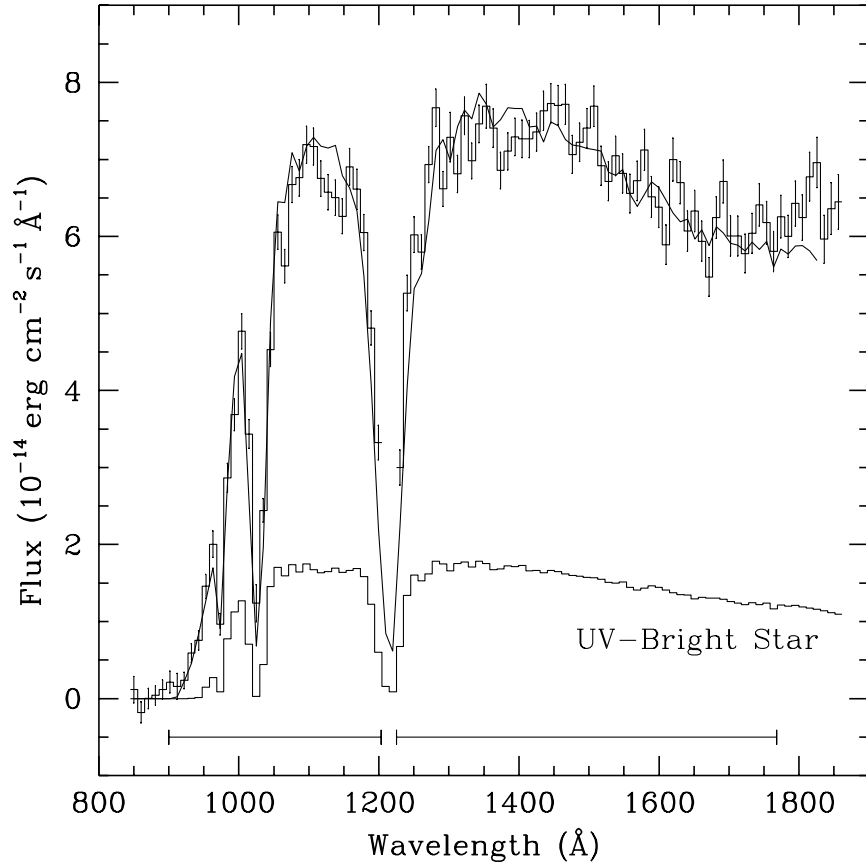


Fig. 5.— HUT spectrum of M79, with error bars. The data have been airglow subtracted and flux calibrated, but not dereddened, and are binned by 20 pixels (about 10 \AA). Overplotted is the best-fitting Gaussian model ($\chi^2 = 307$, $\nu = 81$) drawn from the Lee et al. (1990) mass distribution that best reproduces the optical CMD of M79 (Ferraro et al. 1992; see Sec. 4.1). The model assumes $[M/H] = -1.5$ and includes a UV-bright star with $T_{eff} = 13\,000 \text{ K}$, $\log g = 3.3$, whose spectrum is plotted below. The models have been reddened with a Clayton et al. (1989) extinction curve, assuming $E(B-V) = 0.01$ and $R_V = 3.1$, and include absorption by interstellar hydrogen at a column density of $N_H = 5.307 \times 10^{19} \text{ cm}^{-2}$. Regions used in the fit are indicated by bars at the bottom of the figure.

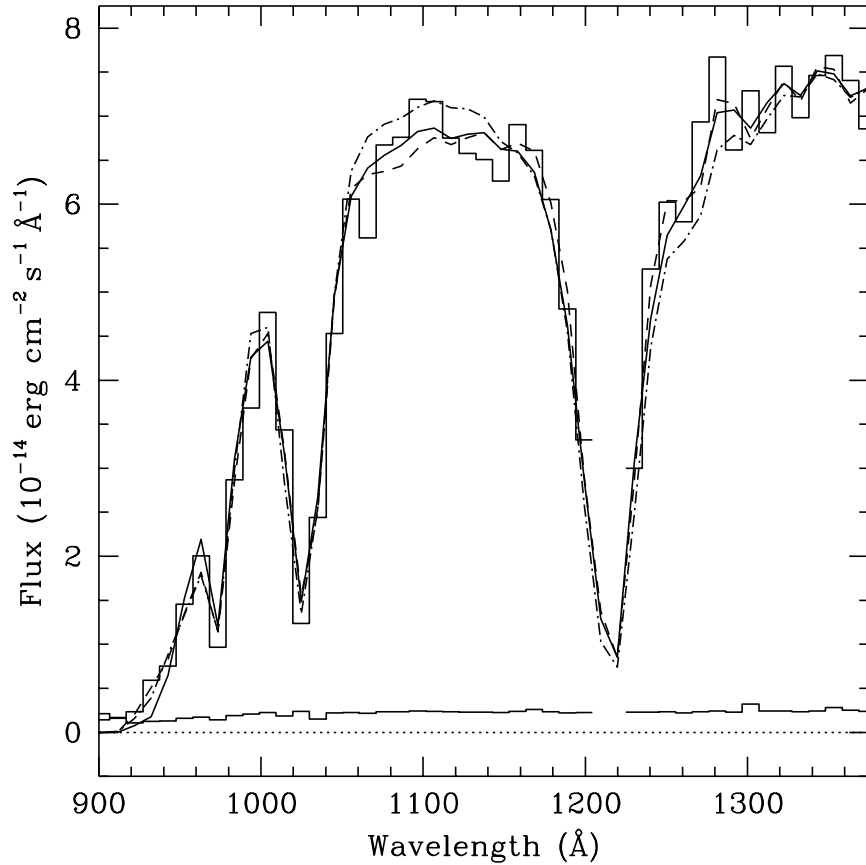


Fig. 6.— HUT spectrum of M79, reduced as in Fig. 5. Overplotted are three simple models, each composed of 4 to 5 individual Kurucz (1992) model spectra. The dashed line is the sum of four spectra, all with $[M/H] = -1.0$, chosen to minimize χ^2 , which equals 148. The solid line is composed of four spectra, each with $[M/H] = -1.5$ but otherwise unconstrained ($\chi^2 = 171$). The dot-dashed line represents a simplified version of our Gaussian model: for each value of $\log g$ between 3.0 and 5.0 (in steps of 0.5 dex), the range of T_{eff} is limited to that present in the Gaussian model. The model assumes $[M/H] = -1.5$ and yields $\chi^2 = 247$. Increases in χ^2 are due primarily to a broadening of the predicted Ly α line. The three models do not differ significantly longward of 1400 Å. All are reddened with a Clayton et al. (1989) extinction curve, assuming $E(B-V) = 0.01$ and $R_V = 3.1$, and include absorption by interstellar hydrogen at a column density of $N_H = 5.307 \times 10^{19} \text{ cm}^{-2}$. Error bars for the data are plotted at the bottom of the figure.

is 176, and the lowest 50 values of χ^2 fall below 207. Excluding the UV-bright star slightly lowers the quality of the resulting fits. We consider this a successful model and shall refer to it as the “empirical model” in the discussion that follows.

The stars in the empirical model have higher metallicity than the general M79 population and a somewhat unusual distribution of surface gravities. Let us investigate these two effects. In Fig. 6, we plot the simple, four-component $[M/H] = -1.0$ model discussed above (dashed line). Note that it seems to reproduce the Ly α absorption feature fairly well. Next we assemble the four Kurucz models with $[M/H] = -1.5$ that best reproduce the data. These models have $T_{eff} = 8500, 11\,000, 15\,000,$ and $29\,000$ K, and $\log g = 3.5, 3.5, 3.0,$ and $3.5,$ respectively. Combined, the spectra yield $\chi^2 = 170.7$ for $\nu = 74$. The resulting spectrum is plotted as a solid line in Fig. 6; its Ly α profile appears somewhat wider than either our previous model or the data.

Finally, we select individual Kurucz models from our Gaussian model. Fig. 7 shows a plot of $\log g$ vs. T_{eff} for the best-fitting Gaussian and empirical models. The differences between the two models are discussed below. At each value of $\log g$ between 3.0 and 5.0, we select values of T_{eff} from the range of temperatures present in the Gaussian model (open circles). All of these stars have $[M/H] = -1.5$. The best-fitting combination has $T_{eff} = 8250, 9500, 13\,000, 16\,000,$ and $31\,000$ K, and $\log g = 3.0, 3.5, 4.0, 4.5,$ and $5.0,$ respectively. $\chi^2 = 247$ for $\nu = 77$. The model is shown in Fig. 6 as a dot-dashed line; its Ly α absorption feature is the widest of the three models. These results suggest that both metallicity and surface gravity may contribute to the poor fit of our Gaussian model.

One may wonder how such small changes in the Ly α line width can produce such large changes in χ^2 . Keep in mind that χ^2 is calculated not from offsets in wavelength but from offsets in flux. Even small changes in the model line widths imply large changes in the predicted flux for fixed wavelengths in the wings of the line. Given our small error bars (shown in Fig. 6), χ^2 is quite sensitive to such discrepancies.

5. Discussion

It appears to us more likely that difficulties in fitting the far-UV spectrum of M79 reflect deficiencies in the model atmospheres than errors in the HB evolutionary models. In many ways, this problem is similar to that found by Moehler et al. (1995), who analyzed low and intermediate-resolution optical spectra of stars along the BHB of M15. They used Kurucz (1992) models of both the Balmer line profiles and the stellar continuum to determine $T_{eff}, \log g,$ and M_* and compared these results with the stellar parameters predicted by Dorman et al. (1991) for evolved HB stars at the metallicity of M15 ($[Fe/H] = -2.17$; Djorgovski 1993). Moehler et al. found that both the stars’ surface gravities and their masses are systematically lower than is predicted for HB stars even when luminosity evolution is accounted for.

Fig. 7 shows a theoretical $\log g - T_{eff}$ diagram. We plot as open circles the stars from the Gaussian model, based on Equation (1) and the Dorman et al. (1993) evolutionary tracks, that best reproduces the HUT spectrum ($\chi^2 = 307$). Plotted as solid circles are the stars from our best-fitting empirical model ($\chi^2 = 176$), based directly on the cluster’s CMD and assuming the $\log g - T_{eff}$ relation derived in Sec.

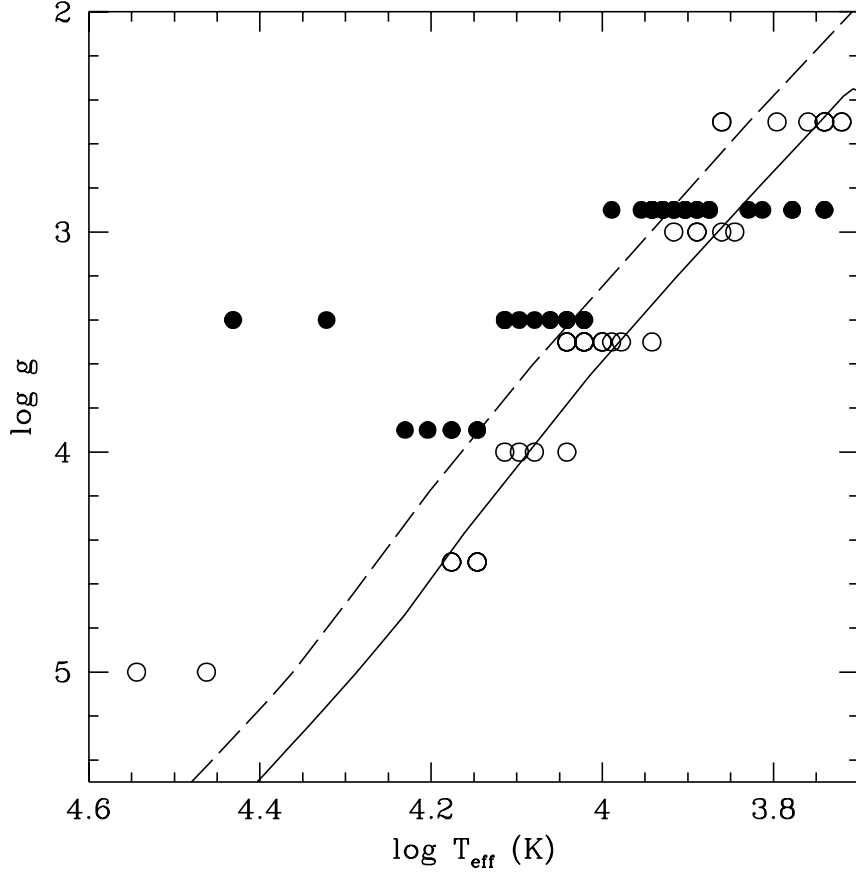


Fig. 7.— A theoretical $\log g - T_{eff}$ diagram. Plotted as open circles are the stars from the Gaussian model, based on Equation (1) and the Dorman et al. (1993) evolutionary tracks, that best reproduces the HUT spectrum ($\chi^2 = 307$). Plotted as solid circles are the stars from our best-fitting empirical model ($\chi^2 = 176$), based directly on the cluster’s CMD and assuming the $\log g - T_{eff}$ relation derived in Sec. 4.2. For clarity, the solid circles have been offset by -0.1 dex in $\log g$. Also plotted are the ZAHB (solid line) and the terminal-age HB (TAHB; dashed line), representing the time of core helium exhaustion, both from Dorman et al. (1993).

4.2. We see that the stars of our empirical model have systematically lower values of $\log g$ at a given effective temperature than do the stars of our Gaussian model. (The stars with $T_{eff} \lesssim 7500$ K, which do not follow this trend, are not constrained by our analysis.) Moehler et al. (1995) found an offset of about 0.2 dex between the predicted and measured surface gravities of HB stars in M15. We also plot in Fig. 7 the ZAHB (solid line) and the terminal-age HB (TAHB; dashed line), which represents the time of core helium exhaustion, both from Dorman et al. (1993). Like Moehler et al., we find that stars in our empirical model tend to lie above the ZAHB and even slightly above the TAHB.

Fig. 8 shows the masses of the stars in our best-fitting empirical model, scaled from the V magnitudes of the cluster’s HB stars. The solid line, again, is the ZAHB of Dorman et al. (1993). Stars with $T_{eff} < 7500$ K are not included in this plot. The masses calculated for these stars are far lower than is predicted by standard HB evolutionary theory. Moehler et al. (1995) determined the masses of several dozen HB stars in six globular clusters using published atmospheric parameters. Their masses range between about 0.2 and 0.5 M_{\odot} at $T_{eff} = 10\,000$ K, also lower than the ZAHB values predicted by Dorman et al. (1991).

In presenting Figs. 7 and 8, we do not pretend to have derived accurate surface gravities and masses for the HB stars in M79 from its optical CMD. Instead, we wish to illustrate how the $\log g - T_{eff}$ relationship assumed by our empirical model differs from that predicted by canonical HB evolutionary theory. The basis for this relationship remains our model fits to the cluster’s far-UV spectrum and the strong sensitivity of χ^2 to changes in the models’ surface gravity observed in Sec. 4.2. We believe that this result indicates a real discrepancy between HB evolutionary theory and the models most commonly used to determine stellar parameters, if not between the theory and the stars themselves.

The high metallicity of the stars in the empirical model may be an artifact of the uncertainties in their surface gravities, or may reflect genuine abundance anomalies in the cluster’s HB stars. In Kurucz’s (1992) model spectra, the apparent far-UV continuum level is determined by the combined absorption of innumerable metal lines. The completeness of the absorption-line models and the relative abundances of the absorbing species determine the shape of the resulting model spectrum. The models assume scaled solar abundances, but this is certainly inappropriate. Giant-branch stars in 47 Tuc ($[Fe/H] = -0.71$; Djorgovski 1993), for example, have non-solar abundance ratios, with enhancements in aluminum and α elements (Brown et al. 1990; Brown & Wallerstein 1992). These abundance anomalies contribute line opacity that is not included in the Kurucz models.

In both the work of Moehler et al. (1995) and in this paper, discrepancies in the hydrogen line widths are responsible for the poor fits at the surface gravities predicted by the evolutionary models: in their work it is the Balmer series, whereas in ours it is the Lyman series. We suggest that improving the treatment of hydrogen absorption in the Kurucz (1992) spectral synthesis codes may help to solve this problem. This is an important task, as it would allow the joint optical/UV technique we have adopted to provide meaningful constraints on the mass distribution of the HB, and the Balmer series line fits to provide accurate masses for individual HB stars. Given the current discrepancies between derived stellar parameters and HB evolutionary theory, however, we conclude that it is not yet possible to combine these models to provide

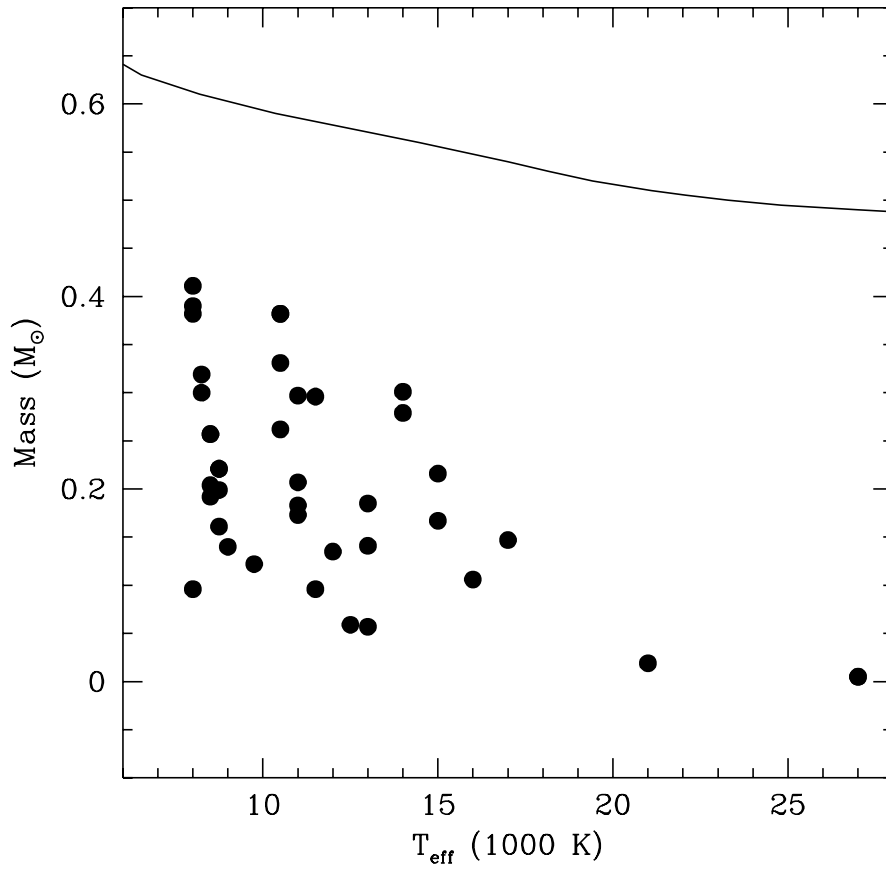


Fig. 8.— The masses of the stars in our best-fitting empirical model, scaled to reproduce the V magnitudes of the HB stars observed by Ferraro et al. (1992). The solid line is the ZAHB of Dorman et al. (1993). Stars with $T_{\text{eff}} < 7500$ K are not included in this plot.

meaningful constraints on the ZAHB mass distribution in globular clusters.

We *can* place limits on the temperature distribution of the HB stars in M79. UIT set an upper limit of 25 000 K to the temperature of stars farther than $1'$ from the cluster center (Hill et al. 1992). The Ferraro et al. (1992) optical CMD contains four stars with $-0.3 < B-V < -0.25$, indicating $27\,000\text{ K} \lesssim T_{eff} \lesssim 32\,000\text{ K}$. While these particular measurements may be uncertain, we find that each of the ten best-fitting synthetic spectra from our empirical model includes a substantial contribution from stars with $T_{eff} \gtrsim 27\,000\text{ K}$. For example, the simple, four-component $[M/H] = -1.0$ model, plotted as a dashed line in Fig. 6, includes a flux contribution from Kurucz models with $T_{eff} = 27\,000\text{ K}$ corresponding to 2.2 ZAHB stars. Only such stars can produce the observed flux shortward of $\text{Ly}\gamma$; thus, at least a few hot stars must reside within about $1'$ of the cluster center. We see no evidence, however, of a large population of previously unobserved extreme HB stars—or of any objects with $T_{eff} \gtrsim 32\,000\text{ K}$.

6. Conclusions

We have shown that the apparently asymmetric distribution of HB stars in M79 observed by Ferraro et al. (1992) can be reproduced with a ZAHB mass-distribution function in the form of a Gaussian with polynomial truncation terms if stellar evolution is properly taken into account. The function that best fits the HB of M79 has a mean mass of $0.59M_{\odot}$ and a standard deviation of $0.05M_{\odot}$. This study represents one of the first detailed investigations into the underlying stellar mass distribution on the HB.

The synthetic HB distribution that best fits the optical CMD is, however, unable to reproduce the HUT far-UV spectrum of the cluster. Kurucz (1992) models fit directly to the HUT spectrum have values of $\log g$ —and thus stellar masses—significantly lower than are predicted by canonical HB evolutionary theory. This result is consistent with the recent report by Moehler et al. (1995) that Kurucz (1992) stellar atmosphere models yield surface gravities for BHB stars systematically lower than are predicted by the evolutionary tracks of Dorman et al. (1991). Kurucz models with $[M/H] = -1.0$ provide significantly better fits to the cluster spectrum than do those with $[M/H] = -1.5$. These discrepancies may reflect non-solar abundances ratios in the HB stars of M79 and/or problems in the treatment of hydrogen absorption by the Kurucz model atmospheres. The deficiencies are made obvious here by the high signal-to-noise ratio of the HUT spectra and the reliability of their calibration.

Stars with $27\,000\text{ K} \lesssim T_{eff} \lesssim 32\,000\text{ K}$ are required to reproduce the observed flux shortward of $\text{Ly}\gamma$. Thus, at least a few such objects must reside within about $1'$ of the cluster center, and should be detectable using WFPC2 on *HST*. We see no evidence, however, of a large population of previously unobserved extreme HB stars.

We would like to thank R. Rood for helpful discussions; W. Landsman for kindly providing a UIT image of M79 (FUV0141NC) and UIT coordinates and magnitudes for the cluster’s HB stars; L. Danly and K. Kuntz for providing a 21-cm spectrum taken in the direction of M79 (Stark et al. 1992); and R. Kurucz for providing a computer-readable tape of his stellar atmosphere models. This research has made use of

the Simbad database, operated at CDS, Strasbourg, France. We wish to acknowledge the efforts of our colleagues on the HUT team as well as the NASA support personnel who helped make the Astro-1 mission successful. The Hopkins Ultraviolet Telescope Project is supported by NASA contract NAS5-27000 to the Johns Hopkins University. BD acknowledges support from NASA RTOP 188-41-51-03.

REFERENCES

- Altner, B., & Matilsky, T. A. 1993, *ApJ*, 410, 116
- Brown, J. A., & Wallerstein, G. 1992, *AJ*, 104, 1818
- Brown, J. A., Wallerstein, G., & Oke, J. B. 1990, *AJ*, 100, 1561
- Cardelli, J. A., Clayton, G. C., & Mathis, J. S. 1989, *ApJ*, 345, 245
- Castellani, V. 1980, in *Globular Clusters*, ed. D. Hanes & B. Madore (Cambridge: Cambridge University Press), 65
- Catelan, M. 1989, *A&AS*, 98, 547
- Daidsen, A. F., et al. 1992, *ApJ*, 392, 264
- Dixon, W. V., Daidsen, A. F., & Ferguson, H. C. 1994, *AJ*, 107, 1388
- Dixon, W. V., Daidsen, A. F., & Ferguson, H. C. 1995, *ApJ*, 454, L47
- Djorgovski, S. 1993, in *ASP Conf. Proc. 50, Structure and Dynamics of Globular Clusters*, ed. S. Djorgovski & G. Meylan (San Francisco: ASP), 373
- Djorgovski, S., & King, I. R. 1986, *ApJ*, 305, L61
- Dorman, B., Lee, Y.-W., & VandenBerg, D. A. 1991, *ApJ*, 366, 115
- Dorman, B., Rood, R. T., & O'Connell, R. W. 1993, *ApJ*, 419, 596
- Ferraro, F. R., Clementini, G., Fusi Pecci, F., Sortino, R., & Buonanno, R. 1992, *MNRAS*, 256, 391
- Fusi Pecci, F., Ferraro, F. R., Bellazzini, M., Djorgovski, S., Piotto, G., & Buonanno, R. 1993, *AJ*, 105, 1145
- Harris, W. E., & Racine, R. 1979, *ARA&A*, 17, 241
- Hill, R. S., et al. 1992, *ApJ*, 395, L17
- Kimble, R. A., et al. 1993, *ApJ*, 404, 663
- Kriss, G. A. 1994, in *ASP Conf. Proc. 61, Astronomical Data Analysis Software and Systems III*, ed. D. R. Crabtree, R. J. Hanisch, & J. Barnes (San Francisco: ASP), 437
- Kruk, J. W., Daidsen, A. F., Durrance, S. T., Kriss, G. A., Buss, R. H., Kimble, R. A., Finley, D., & Holberg, J. B. 1996, in preparation
- Kudritzki, R.-P. 1979, in *Les éléments et leurs isotopes dans l'Univers, Communications présentées au XXII^e Colloque International d'Astrophysique, tenu à Liège (Cointé-Ougrée, Belgium: Université de Liège, Institut d'Astrophysique)*, 295

- Kudritzki, R.-P. 1990, in ASP Conf. Proc. 7, Properties of Hot Luminous Stars, ed. C. D. Garmany (San Francisco: ASP), 315
- Kurucz, R. L. 1992, in IAU Symposium No. 149, The Stellar Populations of Galaxies, ed. B. Barbuy & A. Renzini (Dordrecht: Kluwer), 225
- Lee, Y.-W., Demarque, P., & Zinn, R. 1990, ApJ, 350, 155
- Moehler, S., Heber, U., & de Boer, K. S. 1995, A&A, 294, 65
- Peterson, C. 1993, in ASP Conf. Proc. 50, Structure and Dynamics of Globular Clusters, ed. S. Djorgovski & G. Meylan (San Francisco: ASP), 337
- Press, W. H., Flannery, B. P., Teukolsky, S. A., & Vetterling, W. T. 1988, Numerical Recipes in C (Cambridge: Cambridge University Press), 558
- Renzini, A. 1981, in Effects of Mass Loss on Stellar Evolution, ed. C. Chiosi & R. Stalio (Dordrecht: Reidel), 319
- Rood, R. T. 1973, ApJ, 184, 815
- Rood, R. T. 1990, in The Confrontation between Stellar Pulsation and Evolution, ed. C. Cacciari & G. Clementini (San Francisco: ASP), 11
- Rood, R. T., & Crocker, D. A. 1989, in IAU Colloquium No. 111, The Use of Pulsating Stars in Fundamental Problems of Astronomy, ed. E. G. Schmidt (Cambridge: Cambridge University Press), 103
- Stark, A. A., Gammie, C. F., Wilson, R. W., Bally, J., Linke, R. A., Heiles, C., & Hurwitz, M. 1992, ApJS, 79, 77
- Stetson, P. B., & Harris, W. E. 1977, AJ, 82, 954
- van Albada, T. S., de Boer, K. S., & Dickens, R. J. 1981, MNRAS, 195, 591